Switched-Element Direction Finding

WEI WU

CHARLIE C. COOPER, Member, IEEE

NATHAN A. GOODMAN, Senior Member, IEEE
University of Arizona

We introduce and evaluate the concept of switched-element direction finding. In a switched-element system, simultaneous data collection occurs on only a subset of the array's N elements at any given time. The data collection interval is divided into subintervals, and at each subinterval a multiplexer selects a different subset of $M < N$ elements to connect to the data acquisition channels. Since the switched-element system only collects data on M channels at a time, hardware costs can be reduced at the expense of a time-accuracy tradeoff compared to a full-channel system.

We propose two algorithms. The first is a modification of the root-MVDR (minimum variance distortionless-response) algorithm that is appropriate for linear arrays and noncoherent sources. When sources are coherent, a second algorithm based on a compositely formed full-size covariance matrix is proposed. Although performance depends strongly on the number of sources, good performance can be obtained even when the number of sources is greater than M.

Manuscript received August 16, 2007; revised January 21, 2008; released for publication August 12, 2008.

IEEE Log No. T-AES/45/3/933970.

Refereeing of this contribution was handled by M. Rangaswamy.

Authors' current addresses: W. Wu, Aware, Inc., Bedford, MA; C. C. Cooper and N. A. Goodman, Dept. of Electrical and Computer Engineering, University of Arizona, 1230 E. Speedway Blvd., Tucson, AZ 85721, E-mail: (Goodman@ece.arizona.edu).

I. INTRODUCTION

The typical implementation of a passive RF direction finding (DF) system involves a dedicated signal acquisition channel (receiver, analog-to-digital converter,...) for each element of the antenna array. During the data collection interval, this straightforward implementation simultaneously captures and stores data from all N antennas in the array. When the data collection interval ends, the DF processor analyzes the data and provides estimates of the directions of arrival (DOAs) using a particular algorithm. There are numerous effective techniques for passive DF including maximum likelihood estimation (ML) [1], the minimum variance distortionless-response algorithm (MVDR) [2, 3], mini-norm [4, 5], multiple signal classification (MUSIC) [6–9], and estimation of signal parameters via rotational invariance techniques (ESPRIT) [10, 11]. One common technique employed by these DF algorithms is to form an $N \times N$ sample covariance matrix from the collection of data snapshots. This covariance matrix then forms the basis for further processing. Subarray techniques such as spatial smoothing [12]–[15] also begin with raw data collected simultaneously over the entire array.

In this paper, we propose an alternative system implementation that simultaneously collects data from a subset of $M < N$ antennas [16]. While the total number of antenna elements remains the same, the system possesses only M data acquisition channels as shown in Fig. 1. The data collection interval is divided into subintervals, and at each subinterval a multiplexer selects a different subset of M elements to connect to the acquisition channels. The DF processor stores the snapshots collected by each M-element subarray over its corresponding subinterval, and combines them to provide the required DOA estimates. In this paper, we assume the system switches through every unique combination of M elements during the data collection interval. In general, however, the antenna switching is not required to be this comprehensive. We call the proposed implementation a switched-element system.

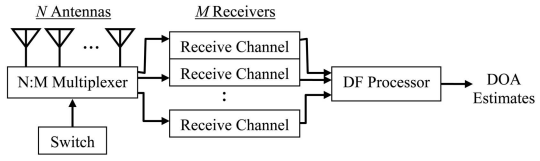

Fig. 1. Block diagram of switched-element DF system.

The primary advantage of the switched-element system is reduced receiver hardware, which implies reduced cost, volume, and weight. Another advantage is the possibility for adaptive switching in response to data collected in prior subintervals. The presence of the switch could also simplify channel calibration

by switching a single antenna to all M receiver chains simultaneously, which would reveal the relative gain and phase responses of the receiver channels in the presence of any incident (even uncooperative) signal. Finally, in some cases the switched-element approach may also require reduced computation and data storage. The compromise, however, is a time-accuracy tradeoff due to less data being gathered compared with a full-array system. Therefore, a balance must be found to satisfy requirements for both hardware cost and accuracy. Given this flexibility, a switched-element system may be desirable in some practical cases.

In this paper, we propose and evaluate two switched-element DF algorithms. First, the root-MVDR technique [1] is extended to be compatible with switched-element direction finding of noncoherent sources. The switched-element root-MVDR algorithm is flexible in that it uses the $M \times M$ sample covariance matrices of all subarrays directly; however, this flexibility also makes it unsuitable for use with coherent sources. For coherent sources, we assemble the full $N \times N$ covariance matrix from components of the individual $M \times M$ covariance matrices. This composite covariance matrix (CCM) can be used with traditional spatial smoothing and MUSIC to resolve multiple coherent signal sources.

The paper is organized as follows. Section II defines our narrowband signal model and problem statement. Section III presents the two switched-element DF algorithms mentioned above. Simulation results are presented and discussed in Section IV, and Section V contains our conclusions.

II. PROBLEM FORMULATION

A. Signal Model

In the narrowband signal model for array processing, far-field sources arriving at the antenna array produce a set of phase shifts across the antenna elements. The relative phase shift for an antenna element located at coordinates (x_n, y_n) is

$$\varphi_n = -k_x x_n - k_y y_n = -\mathbf{k}(\theta) \cdot \mathbf{r}_n \tag{1}$$

where $\mathbf{k}$ is the wavenumber vector with components related to the source DOA by $k_x = k_0 \sin\theta$ and $k_y = k_0 \cos\theta$, $\mathbf{r}_n$ is the antenna element position vector, and $k_0 = 2\pi f_0/c$ is the wavenumber in radians/meter at the source's center frequency f_0 (c is the wave's propagation speed). Defining the array manifold vector for an N-element array as

$$\mathbf{a}(\theta) = [\exp(-j\mathbf{k}(\theta) \cdot \mathbf{r}_1) \quad \exp(-j\mathbf{k}(\theta) \cdot \mathbf{r}_2) \cdots \exp(-j\mathbf{k}(\theta) \cdot \mathbf{r}_N)]^{\mathrm{T}} \tag{2}$$

where $(\cdot)^{\mathrm{T}}$ is the transpose operator, the signal received by the array due to a single source is $s_1(\kappa)\mathbf{a}(\theta)$ where $s_1(\kappa)$ is the signal amplitude at temporal sample index κ. Adding receiver noise and allowing for D sources, the signal model for the data snapshot at time index κ is [1, 17]

$$\mathbf{z}_\kappa = \mathbf{A}\mathbf{s}_\kappa + \mathbf{w}_\kappa \tag{3}$$

where

$$\mathbf{A} = [\mathbf{a}(\theta_1) \quad \mathbf{a}(\theta_2) \cdots \mathbf{a}(\theta_D)] \tag{4}$$

$$\mathbf{s}_\kappa = [s_1(\kappa) \quad s_2(\kappa) \cdots s_D(\kappa)]^{\mathrm{T}} \tag{5}$$

and $\mathbf{w}_\kappa$ is additive spatially and temporally white complex Gaussian noise (AWGN) with unit power. We assume that the signals are zero-mean complex Gaussian random processes; therefore, each $s_d(\kappa)$ (the dth source's signal amplitude at sample index κ) is a complex zero-mean Gaussian random variable. We assume that snapshots collected at different times are independent and identically distributed. Between signals, however, we consider both the correlated and uncorrelated cases. The signal covariance matrix, $\mathbf{S} = \mathrm{E}[\mathbf{s}_\kappa \mathbf{s}_\kappa^{\mathrm{H}}]$, therefore, is a Hermitian matrix whose dth diagonal entry is the average power P_d of the dth source. Given the normalization of noise power to one, the signal-to-noise ratio (SNR) of the dth source at the output of a given antenna element is $\mathrm{SNR}_d = P_d/1 = P_d$. This is the SNR definition used for all results presented in this paper. For the uncorrelated signal case, the signal covariance matrix is a diagonal matrix. When the signal amplitude coefficients are correlated, the signal covariance matrix has non-zero values off the main diagonal. When signal amplitude coefficients are perfectly correlated, such as when $s_i(\kappa) = \alpha s_j(\kappa)$ for some constant α and $i \neq j$, we say the signals are coherent.

Algorithms such as MVDR and MUSIC typically require data from all N sensors throughout the data collection process for all snapshots. In this paper, however, we focus on the premise that only M channels of data can be collected at any given time. Consequently, we define $\mathbf{z}_\kappa^q$ as the length-M data snapshot formed by extracting M elements from the full-array data vector where the superscript q denotes the qth subarray of the switching operation. In other words, a different subset of M elements is extracted for each value of q. We also define K_q to be the number of (still independent) snapshots collected in the qth switching configuration and Q to be the number of unique configurations.

The problem can now be stated as follows. We assume that only M channels of data can be collected simultaneously, but that a multiplexer allows different subsets of M antennas to be passed to the data acquisition hardware at different times. Our goal is to develop and analyze algorithms for estimating the DOAs of incoming sources. Although we know the hardware cost can be reduced, the switched-element structure causes unique processing issues. First, while

most DF algorithms are based on a single $N \times N$ sample covariance matrix, the switched concept is only capable of producing Q different $M \times M$ sample covariance matrices with different underlying subarray structures. Therefore, we must either modify existing algorithms to accept multiple mismatched $M \times M$ covariance matrices or we must construct the full size covariance matrix by piecing together data gathered from multiple subarrays. Second, the switched-element system collects less data than the full-array system over the same amount of time. This results in a compromise whereby performance of the switched-element system is reduced in comparison to a full-array system when the two systems have equal data collection intervals. Full-array performance can usually be achieved, however, if the switched-element system is allowed to collect data over a longer time interval. Hence, we also quantify the time-accuracy tradeoff inherent in the switched-element concept.

B. Cramer-Rao Bounds

Since the noise and signal samples are Gaussian, the observed data (for the full array) are also Gaussian with covariance matrix

$$\mathbf{K}_z = \mathrm{E}[\mathbf{z}_\kappa \mathbf{z}_\kappa^{\mathrm{H}}] = \mathbf{K}_s(\boldsymbol{\theta}) + \mathbf{I}_N = \mathbf{A}\mathbf{S}\mathbf{A}^{\mathrm{H}} + \mathbf{I}_N \tag{6}$$

where $\boldsymbol{\theta}$ is a vector of unknown source DOAs, $\mathbf{I}_N$ is the $N \times N$ identity matrix, and $(\cdot)^{\mathrm{H}}$ is the conjugate-transpose operator. Therefore, the pdf of the κth data snapshot is

$$p(\mathbf{z}_\kappa;\boldsymbol{\theta}) = \frac{1}{|\pi \mathbf{K}_z|} \exp(-\mathbf{z}_\kappa^{\mathrm{H}} \mathbf{K}_z^{-1} \mathbf{z}_\kappa). \tag{7}$$

Given the independence of successive samples of signal and noise, the pdf for a full collection of K snapshots is

$$p(\mathbf{z}_1, \mathbf{z}_2, \ldots, \mathbf{z}_K;\boldsymbol{\theta}) = \prod_{\kappa=1}^{K} \frac{1}{|\pi \mathbf{K}_z|} \exp(-\mathbf{z}_\kappa^{\mathrm{H}} \mathbf{K}_z^{-1} \mathbf{z}_\kappa). \tag{8}$$

According to [1], the Fisher information matrix (FIM) for this scenario is

$$\mathbf{J}_{\theta\theta} = 2K\mathrm{Re}\left\{ \begin{array}{l} [\mathbf{S}\mathbf{A}^{\mathrm{H}}\mathbf{K}_z^{-1}\mathbf{M}] \odot [\mathbf{S}\mathbf{A}^{\mathrm{H}}\mathbf{K}_z^{-1}\mathbf{M}]^{\mathrm{T}} \\ +[\mathbf{S}\mathbf{A}^{\mathrm{H}}\mathbf{K}_z^{-1}\mathbf{A}\mathbf{S}] \odot [\mathbf{M}^{\mathrm{H}}\mathbf{K}_z^{-1}\mathbf{M}]^{\mathrm{T}} \end{array} \right\} \tag{9}$$

where $\odot$ is the Hadamard matrix product, $\mathrm{Re}\{\cdot\}$ denotes the real part of a complex number, and $\mathbf{M}$ is

$$\mathbf{M} = \left[\frac{\partial \mathbf{a}(\theta_1)}{\partial \theta_1} \quad \frac{\partial \mathbf{a}(\theta_2)}{\partial \theta_2} \cdots \frac{\partial \mathbf{a}(\theta_N)}{\partial \theta_N} \right]. \tag{10}$$

The Cramer-Rao (CR) bound is defined by $\mathbf{C}(\boldsymbol{\theta}) = \mathbf{E}[(\hat{\boldsymbol{\theta}} - \boldsymbol{\theta})(\hat{\boldsymbol{\theta}} - \boldsymbol{\theta})^{\mathrm{T}}] \geq \mathbf{J}_{\theta\theta}^{-1}$ where the inequality is used to indicate that $\mathbf{C}(\boldsymbol{\theta}) - \mathbf{J}_{\theta\theta}^{-1}$ is a nonnegative definite matrix [1].

A switched-element system collects data using Q sequential subarray configurations. First, the system connects the receiver inputs to the outputs of the M antenna elements in the first subarray configuration. The system stays in this configuration long enough to collect K_1 independent data snapshots (in the same manner as the full-array system above collects K independent snapshots, but the switched system collects data from M elements instead of N). When the K_1 snapshots are collected, the system switches the receiver inputs to a new set of M antenna outputs and collects K_2 snapshots in this configuration. When this is done, the system switches again and collects K_3 snapshots from a third unique subarray configuration. This process continues until data collection from the Qth subarray configuration is complete.

All snapshots are collected sequentially in time such that signal amplitude and noise fluctuations are independent, even for snapshots collected by the same subarray. However, the spatial covariance matrix varies depending on the structure of a particular subarray. Define

$$\mathbf{K}_z^q = \mathrm{E}[\mathbf{z}_\kappa^q (\mathbf{z}_\kappa^q)^{\mathrm{H}}] = \mathbf{A}_q \mathbf{S} \mathbf{A}_q^{\mathrm{H}} + \mathbf{I}_M \tag{11}$$

as the covariance matrix for the qth array configuration where

$$\mathbf{A}_q = [\mathbf{a}_q(\theta_1) \quad \mathbf{a}_q(\theta_2) \cdots \mathbf{a}_q(\theta_D)] \tag{12}$$

is the array manifold matrix valid for the qth subarray. Noting that the qth configuration is formed using a subset of M elements from the full array, we see that the elements of $\mathbf{a}_q(\theta)$ are equal to the elements of the full-array manifold vector $\mathbf{a}(\theta)$ that correspond to the elements in the subarray. For example, suppose $M = 3$ and the first, third, and fourth antenna elements of the full array are selected for the qth subarray, then $\mathbf{a}_q(\theta)$ is formed by taking the first, third, and fourth entries of $\mathbf{a}(\theta)$. Furthermore, the 3×3 covariance matrix $\mathbf{K}_z^q$ will have entries equal to the corresponding entries of the full-array covariance matrix $\mathbf{K}_z$. In this case, the $(2,1)$ entry of $\mathbf{K}_z^q$ is equal to the $(3,1)$ entry of $\mathbf{K}_z$ because both values describe the correlation between the same two antenna elements. This relationship will be exploited in Section IIIB where we use switched-element data to approximate a full-array covariance matrix for use with spatial smoothing.

The joint pdf of the snapshot vectors for the switched-element system is

$$p(\mathbf{z}_1^1, \mathbf{z}_2^1, \ldots, \mathbf{z}_{K_Q}^Q;\boldsymbol{\theta}) = \prod_{q=1}^{Q} \prod_{\kappa=1}^{K_q} \frac{1}{|\pi \mathbf{K}_z^q|} \exp[-(\mathbf{z}_\kappa^q)^{\mathrm{H}} (\mathbf{K}_z^q)^{-1} (\mathbf{z}_\kappa^q)]. \tag{13}$$

The FIM for a single subarray configuration pair takes the same form as (9), but with the array manifold and covariance matrix appropriate to that

subarray:

$$\mathbf{J}_{\theta\theta}^{q} = 2K_q \mathrm{Re}\left\{ \begin{array}{l} [\mathbf{S}\mathbf{A}_q^{\mathrm{H}}(\mathbf{K}_z^q)^{-1}\mathbf{M}_q] \odot [\mathbf{S}\mathbf{A}_q^{\mathrm{H}}(\mathbf{K}_z^q)^{-1}\mathbf{M}_q]^{\mathrm{T}} \\ +[\mathbf{S}\mathbf{A}_q^{\mathrm{H}}(\mathbf{K}_z^q)^{-1}\mathbf{A}_q\mathbf{S}] \odot [\mathbf{M}_q^{\mathrm{H}}(\mathbf{K}_z^q)^{-1}\mathbf{M}_q]^{\mathrm{T}} \end{array} \right\}. \tag{14}$$

Based on the independence between snapshots collected by different subarrays, the total FIM is the sum of the individual FIMs for each subarray [1]; therefore, the CR bound for the switched-element system is

$$\mathbf{C}^{sw}(\boldsymbol{\theta}) \geq (\mathbf{J}_{\theta\theta}^{sw})^{-1} \tag{15}$$

where $\mathbf{J}_{\theta\theta}^{sw} = \sum_{q=1}^{Q} \mathbf{J}_{\theta\theta}^{q}$.

Since the switched system's total FIM is a sum of individual FIMs, and the individual FIMs are scaled by the number of snapshots for that subarray, we note that the CR bound varies depending on how the total data collection time is allocated to the different subarrays—in other words, through the selection of the K_q's. It is interesting to consider whether the CR bound can be used to optimally allocate a finite number of snapshots across the individual subarray configurations. Unfortunately, since the CR bound is a local error measure [1, 18], optimal allocation in terms of the CR bound would assign all snapshots to the subarray configuration with the widest baseline since it will have the best angular resolution. While this approach will minimize the CR bound, we must consider that subarrays are formed by selecting a subset of antennas from the full array. This implies that individual subarrays will be undersampled, and switching between a variety of different subarrays with different spatial configurations is essential for avoiding ambiguity-type errors. Hence, allocating snapshots to the individual subarray configurations is a compromise between making global errors and reducing the variance of local errors.

In Section III, two algorithms are proposed. The first one involves the direct processing of a set of $M \times M$ sample covariance matrices. This algorithm works well for uncorrelated signals. When the signal amplitude coefficients are correlated, the rank of the signal covariance matrix degenerates to a value less than the number of sources D. This is known to affect covariance-based DF algorithms significantly, but in certain situations the spatial smoothing technique can restore much of the performance. Spatial smoothing, however, requires two or more identically structured subarrays that differ only by a shift in position. While in some cases the subarray corresponding to a particular switch configuration could be partitioned even further for the purpose of spatial smoothing, the subarray structure of the different switched-element configurations is not guaranteed to support this in general. Hence, our second algorithm forms a composite full size matrix, and by incorporating the spatial smoothing technique, it can deal with coherent signal sources.

III. DF ALGORITHMS FOR A SWITCHED-ELEMENT ARRAY

A. Switched-Element Root-MVDR Algorithm

As mentioned above, most DF algorithms are based on the sample covariance matrix (SCM), which for the full array of N elements is formed by

$$\mathbf{R}_z = \frac{1}{K}\sum_{\kappa=1}^{K} \mathbf{z}_\kappa \mathbf{z}_\kappa^{\mathrm{H}} \tag{16}$$

where K is the total number of snapshots. The MVDR spectrum [2] is given by

$$\hat{P}_{\mathrm{mvdr}}(\theta) = \frac{1}{\mathbf{a}^{\mathrm{H}}(\theta)\mathbf{R}_z^{-1}\mathbf{a}(\theta)} \tag{17}$$

where $\mathbf{a}(\theta)$ is defined in (2). Peaks in $\hat{P}_{\mathrm{mvdr}}(\theta)$ indicate source DOAs.

In a switched-element system, however, we cannot form the full SCM directly. Alternatively, we can find the SCM for each switch configuration, which for the qth configuration is

$$\mathbf{R}_z^q = \frac{1}{K_q}\sum_{\kappa=1}^{K_q} \mathbf{z}_\kappa^q (\mathbf{z}_\kappa^q)^{\mathrm{H}}. \tag{18}$$

To obtain a switched-element MVDR algorithm, we define a spectrum that incorporates all Q configurations according to

$$\hat{P}_{SW}(\theta) = \frac{1}{\sum_{q=1}^{Q} \mathbf{a}_q^{\mathrm{H}}(\theta)(\mathbf{R}_z^{\mathrm{q}})^{-1}\mathbf{a}_q(\theta)}. \tag{19}$$

Defining the first element in each switch configuration as the reference element for that subarray, the manifold vector $\mathbf{a}_q(\theta)$ is

$$\mathbf{a}_q(\theta) = [1 \quad e^{-j\mathbf{k}(\theta)\cdot(\mathbf{r}_2^q - \mathbf{r}_1^q)} \cdot e^{-j\mathbf{k}(\theta)\cdot(\mathbf{r}_M^q - \mathbf{r}_1^q)}]^{\mathrm{T}} \tag{20}$$

where $\mathbf{r}_i^q$ is the position vector of the ith element in the qth subarray. Note that $\mathbf{R}_z^q$ is always $M \times M$ and $\mathbf{a}_q(\theta)$ is $M \times 1$. By evaluating over all θ, we can estimate the DOAs by finding the D maxima in the spectrum. This is the spectral version of the switched-element MVDR algorithm.

The root-MVDR algorithm is an efficient method to evaluate the MVDR kernel [1]. Rather than maximizing (17), the root-MVDR algorithm uses a polynomial root-finding approach to minimize the denominator of (17), but for the switched-element concept, we apply the polynomial root-finding technique to find the minima of the denominator of (19). If the antenna array is linear with all elements located at integer multiples of a fundamental spacing d_0, then the array manifold vector for the qth subarray (referenced to the first element of the subarray) is

$$\mathbf{a}_q(\theta) = [1 \quad e^{-jk_x(m_2^q - m_1^q)d_0} \cdots e^{-jk_x(m_M^q - m_1^q)d_0}]^{\mathrm{T}} \tag{21}$$

where m_i^q is an integer that defines the location of the ith element of the qth subarray in terms of the fundamental spacing. Defining $b = \exp(jk_x d_0)$, the array manifold vector becomes

$$\mathbf{a}_q(\theta) = [1 \quad b^{-(m_2^q - m_1^q)} \cdots b^{-(m_M^q - m_1^q)}]^{\mathrm{T}} \tag{22}$$

which consists of integer powers of the variable b. Letting $\mathbf{G}_q = (\mathbf{R}_z^q)^{-1}$, the denominator of (19) is

$$\hat{L}(\theta) = \frac{1}{\hat{P}_{SW}(\theta)} = \sum_{q=1}^{Q} \mathbf{a}_q^{\mathrm{H}}(\theta)\mathbf{G}_q\mathbf{a}_q(\theta). \tag{23}$$

To see that (23) is a polynomial, consider the $M = 2$ case. Letting

$$\mathbf{G}_q = \begin{bmatrix} g_{11}^q & g_{12}^q \\ g_{21}^q & g_{22}^q \end{bmatrix} \tag{24}$$

we have

$$\mathbf{a}_q^{\mathrm{H}}\mathbf{G}_q\mathbf{a}_q = g_{11}^q + g_{12}^q b^{-(m_2^q - m_1^q)} + g_{21}^q b^{(m_2^q - m_1^q)} + g_{22}. \tag{25}$$

Substituting (25) into (23), we obtain

$$\hat{L}(\theta) = \sum_{q=1}^{Q} (g_{11}^q + g_{12}^q b^{-(m_2^q - m_1^q)} + g_{21}^q b^{(m_2^q - m_1^q)} + g_{22}^q) \tag{26}$$

which is also a polynomial. At this point, we can use an efficient polynomial rooting algorithm to find the minima of (26). Note, however, that the definition of b above implies that roots corresponding to sinusoidal plane waves should have unit magnitude. Therefore, the roots of (26) closest to the unit circle are the ones that correspond to propagating sources, and the DOA estimates are obtained by setting the phase of the root equal to $k_x d_0$. Furthermore, since $\hat{L}(\theta)$ is conjugate symmetric, each root of (26) has a conjugate reciprocal root. Hence, we only need to examine either the roots inside the unit circle or outside the unit circle, but not both.

One advantage of the switched root-MVDR algorithm is its compatibility with the switched-element concept. Since the switched root-MVDR algorithm works directly on the $M \times M$ covariance matrices of the individual subarrays, we are not required to include every antenna pair in the switching pattern. By contrast, if an individual antenna element is to be included in the CCM (described below), the switching pattern must ensure that sometime during the data collection this antenna is "on" at the same time as each of the other antennas in the array. Otherwise, elements of the full covariance matrix will be missing. Unfortunately, this places a constraint on the switching pattern that may not be consistent with best performance. For example, if input SNR is well above the threshold SNR [1] such that ambiguity-type errors are unlikely, it would benefit the system to collect more snapshots with large antenna baselines to refine the angle estimate(s) rather than smaller baselines that prevent ambiguity errors. The switched root-MVDR algorithm is consistent with this desired flexibility.

One disadvantage of the root-MVDR algorithm, however, is its inability to handle coherent sources. Because the algorithm operates on multiple $M \times M$ covariance matrices formed from subarrays with different structures, the spatial smoothing technique cannot be applied directly. The switched-element root-MVDR algorithm works well for noncoherent sources, but when coherent signals are known to be present, we propose the CCM-based root-MUSIC algorithm described next.

B. CCM-Based Root-MUSIC with Spatial Smoothing

Spatial smoothing requires two or more identically structured subarrays that differ only by a shift in position. While the switched-element system could certainly select different subsets of M antennas with the same subarray structure (assuming the full array has the proper structure to begin with), the data collected by these different subsets must be collected at different times. Therefore, the signal coefficient realizations (the $s_d(\kappa)$'s) are different for each subarray, which leads to poor results for the switched root-MVDR algorithm. Although the CCM is also formed from data snapshots containing different signal coefficient realizations, the CCM-based root-MUSIC technique is less sensitive to this difficulty.

For a given subset of antennas, the $M \times M$ SCM is

$$\mathbf{R}_z^q = \begin{bmatrix} \sigma_{11}^q & \sigma_{12}^q & \cdots & \sigma_{1M}^q \\ \sigma_{21}^q & \sigma_{22}^q & & \vdots \\ \vdots & & \ddots & \\ \sigma_{M1}^q & \cdots & & \sigma_{MM}^q \end{bmatrix} \tag{27}$$

where σ_{ij}^q is the sample correlation between the ith and jth antennas of the qth subarray. If the system collects and stores data from all combinations of antennas, the full-dimension $N \times N$ CCM can be constructed by substituting entries from the individual $\mathbf{R}_z^q$ in (21). For example, if the ith and jth antennas of the qth subarray are the same as the mth and nth antennas of the full array, respectively, then we can set $\tilde{\mathbf{R}}_z(m,n) = \mathbf{R}_z^q(i,j)$ where $\tilde{\mathbf{R}}_z$ is the CCM. Since the data from each subarray configuration are independent, repeated measurement of the variances (diagonal entries) can be averaged to make full use of the collected data (however, this seems to have little performance benefit). The CCM has the same form as a regular SCM; therefore, given an array with proper structure, we can apply the spatial smoothing technique to resolve correlated sources. For simplicity, in the next section we assume a fully populated linear array for all simulations involving coherent sources.

An interesting characteristic of the CCM is that it is not positive definite, which we expect from a proper covariance matrix. This characteristic occurs because different elements of the CCM are estimated from data collected at different times. Since the data are collected at different times, the signal coefficient realizations are different. This creates an inconsistency that manifests itself as real, negative eigenvalues. Unfortunately, this characteristic prohibits applying the root-MVDR algorithm to the CCM. The MUSIC algorithm requires only the eigenvectors of the smoothed CCM; therefore, the MUSIC algorithm is unaffected by negative eigenvalues. Once the CCM is formed, we apply the root-MUSIC algorithm in the same way that we would for a traditionally formed SCM.

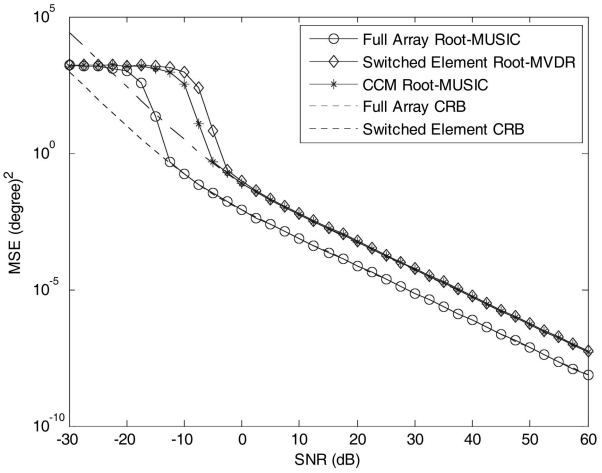

Fig. 2. DF performance for full-array root-MUSIC, switched-element root-MVDR, and CCM root-MUSIC algorithms. One signal impinging from 5 deg.

IV. PERFORMANCE AND ANALYSIS

In this section we evaluate the performance and behavior of switched-element direction finding. The above algorithms are tested against single- and multiple-signal cases. For multiple signals, both coherent and noncoherent cases are considered. Unless otherwise noted, a linear array comprised of $N = 8$ elements is used to estimate the DOA(s). In some simulations, the array elements are uniformly spaced; in others they are sparsely spaced on a uniform grid. For the switched implementation, we assume that the system collects $M = 2$ channels of data at any given time. Therefore, there are $Q = N(N-1)/2 = 28$ unique antenna pair combinations. We assume that the system switches through all 28 combinations and collects an equal number of snapshots for each pair.

In order to make a proper comparison, it is necessary to define the relative amounts of data collected by the full and switched implementations. Possible scenarios include collecting the same total number of snapshots, the same total amount of data, or collecting the same number of snapshots on each subarray configuration as the full-array system collects. When the switched and full-array implementations collect the same total number of snapshots, the collection time interval is the same. Therefore, this comparison shows the performance sacrificed by collecting data on $M < N$ antennas simultaneously.

First, we compare the performance of the switched-element system to a full, nonswitched system for a single source. The source arrives from five degrees relative to the array normal. The system collects 20 snapshots for each antenna pair, resulting in $20 * 28 = 560$ total snapshots. The full array system also collects 560 snapshots. Because the switched-element system collects only two channels of data rather than eight for each snapshot, the total amount of data gathered by the switched-element system is one-fourth of the data collected by the full-array system. We use the root-MUSIC algorithm for the full-array data. Fig. 2 shows the mean-squared error performance and CR bounds for the full-array and switched-element systems. Both switched-element algorithms perform similarly for a single source while the full-array system obviously performs the best due to collecting the most data. The performance of the full-array system approaches the CR bound at lower SNR than the switched system and has smaller error for the same input SNR.

Results in [16] show that the full and switched systems perform similarly if the total data collected is equal rather than the number of snapshots (in this case, for example, the equal-data equivalence would require the switched system to collect 80 snapshots per antenna pair). In general, the switched system can achieve the same single-source performance as the full-array system with an increase in data collection time of approximately N/M. Considering hardware costs, the time-performance tradeoff of a switched-element system may be an acceptable compromise.

Next, we estimate the DOAs of two noncoherent signals arriving from 10 and 55 deg. Because the signals are noncoherent, we can use a nonredundant [18] linear array. In Fig. 3, we notice that the switched-element root-MVDR algorithm outperforms the CCM root-MUSIC algorithm (Figs. 3–6 show the mean-squared error performance of locating the source at 10 deg in the presence of the other sources, not an average over the different sources). This pattern of performance has been tested over various multiple-source (noncoherent) scenarios with the root-MVDR algorithm consistently outperforming CCM-based root music.

Another interesting aspect seen in Fig. 3 is the floor observed for the switched-element algorithms as well as in the CR bound. This floor is a consequence of the fact that the number of sources is equal to

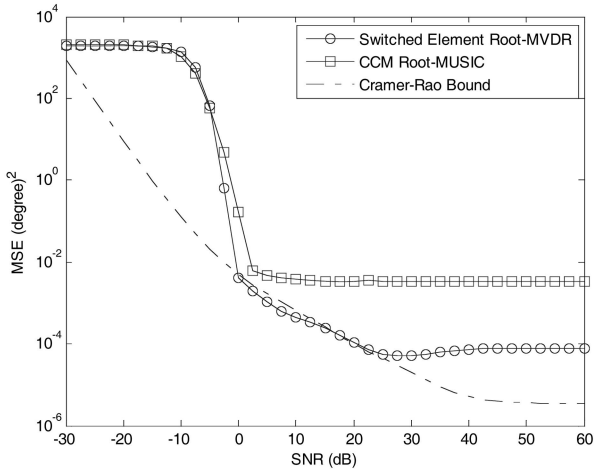

Fig. 3. DF performance for switched-element root-MVDR and CCM root-MUSIC algorithms. Two noncoherent signals arriving from 10 and 55 deg.

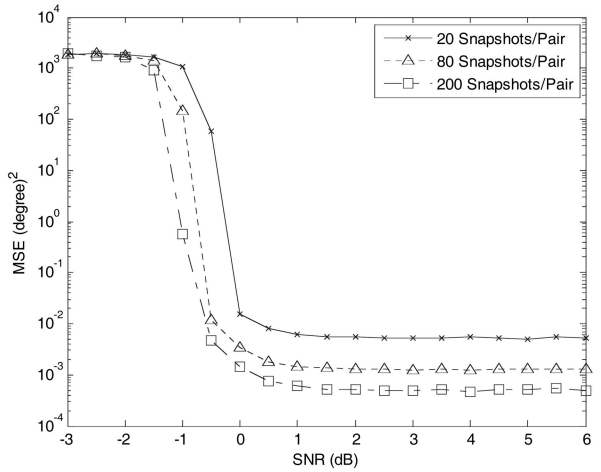

Fig. 4. Performance of CCM root-MUSIC for two noncoherent sources parameterized by number of snapshots.

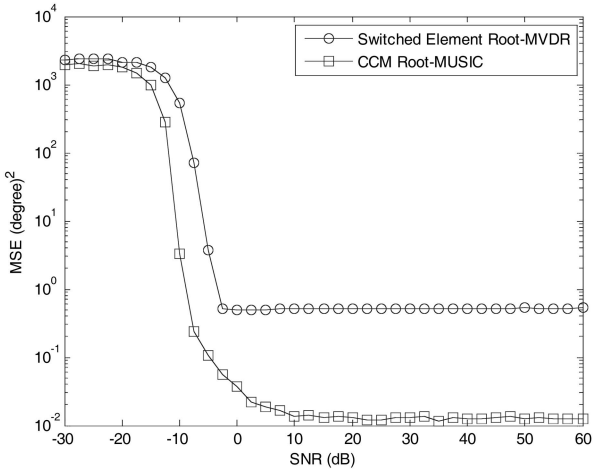

Fig. 5. DF performance for switched-element root-MVDR and CCM root-MUSIC algorithms, with two perfectly correlated signals impinging from 10 and 55 deg.

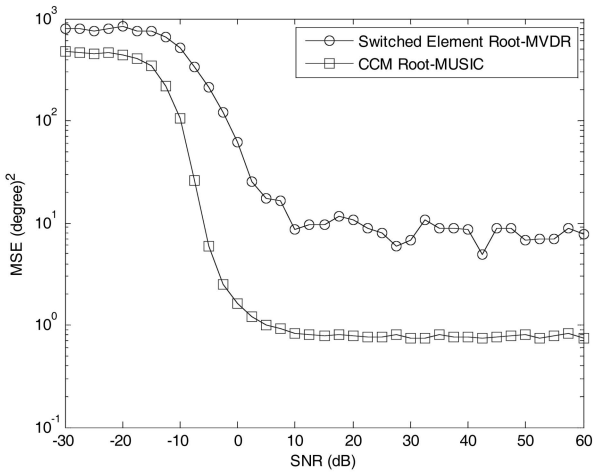

Fig. 6. DF performance for switched-element root-MVDR and CCM root-MUSIC algorithms, with three perfectly correlated signals impinging from -40, 10, and 55 deg.

the number of simultaneous receiving channels. A full-array system has the same behavior, but it is rarely seen because the number of signal sources is rarely equal to the number of antenna elements. One explanation for this behavior can be obtained by considering the way in which training data and SNR affect estimation of the signal-plus-noise and noise-only subspaces of a covariance matrix. At high SNR, the signal-plus-noise subspace is defined mostly by the array manifold vectors and powers of the arriving sources. As SNR increases, it becomes easier to accurately define and separate the signal-plus-noise and noise-only subspaces. The amount of training data will still control how accurately the internal structure of the signal-plus-noise subspace is estimated (and, therefore, the accuracy of DOA estimates), but the span of the subspace will be accurate. Hence, performance constantly improves with increasing SNR, especially if the number of sources is much smaller than the size of the covariance matrix.

When the number of sources is equal to the size of the covariance matrix, the noise-only subspace does not exist. Therefore, we only need to estimate the structure of the matrix, but this depends strongly on the amount of training data because it is necessary to average out signal amplitude fluctuations. Even if the noise power is low, accurate angle estimation requires accurate estimation of the array manifold vectors in the proper proportions of power. This estimation depends on the amount of available training data, not on SNR. Hence, when the number of sources is equal to the size of the covariance matrix, performance eventually achieves a floor where performance is flat with increasing SNR. The MUSIC algorithm, for example, relies on finding valid array manifold vectors that are orthogonal to the noise-only subspace. If the noise-only subspace cannot be accurately defined, performance of the algorithm suffers. Since the switched-element system of Fig. 3 consists of

two-element subarrays, the performance floor can be observed when only two signals are present. If the floor is unacceptable, the number of elements in each switching configuration must be increased. Fig. 4 demonstrates the relationship between snapshots and the performance floor for the CCM root-MUSIC algorithm.

The switched-element root-MVDR algorithm provides good results for noncoherent signals. However, we cannot effectively apply the switched root-MVDR algorithm to coherent signals. The spatial smoothing technique is essential for the estimation of coherent signals and multiple identical subarrays are needed before we can implement the algorithm. In the following simulations, we compare the switched-element root-MVDR and CCM-based root-MUSIC algorithms using a 16-element uniform linear array. Spatial smoothing is applied to the CCM.

Fig. 5 shows simulated results for two perfectly coherent signals arriving from 10 and 55 deg. The spatially smoothed version of CCM root-MUSIC clearly performs the best, which is not surprising since the switched-element root-MVDR algorithm operates directly on 2×2 covariance matrices without spatial smoothing.

Next, we simulate three perfectly correlated signals impinging from -40, 10, and 55 deg. Results shown in Fig. 6 indicate that CCM root-MUSIC continues to provide better performance than switched-element root-MVDR. In comparing Fig. 6 to Fig. 5, we see that mean-squared error has increased significantly due to the presence of an additional source; however, it is encouraging that we are able to obtain modest performance despite the presence of three correlated signals and only two elements per switch configuration.

V. CONCLUSIONS

We have proposed two algorithms for direction finding with a switched-element system. The time-accuracy tradeoff is clear: we cannot achieve the same performance as a full-array system for the same collection time since the switched system collects less data. The advantage of a switched-element system is that only $M < N$ receiving channels are needed; therefore, reduced hardware cost could outweigh the sacrifice in performance. We have demonstrated that well-known DF algorithms such as root-MVDR, root-MUSIC, and spatial smoothing can be adapted to work with a switched-element system. Our results show that switched-element root-MVDR performs well when the signal sources are uncorrelated. On the other hand, if coherent signals are present, the CCM-based root-MUSIC with spatial smoothing appears to be the best choice. As in traditional direction finding, performance can be improved by collecting more data snapshots and/or by increasing the size of the antenna array. For noncoherent sources, the size of the array can be increased by using a nonredundant array, which integrates very well with the switched-element approach.

REFERENCES

[1] Van Trees, H. L.
Optimum Array Processing.
New York: Wiley, 2002.

[2] Capon, J.
High-resolution frequency-wavenumber spectrum analysis.
Proceedings of the IEEE, **57** (Aug. 1969), 1408–1418.

[3] Lacoss, R. T.
Data adaptive spectral analysis methods.
Geophysics, **36** (1971), 661–675.

[4] Reddi, S. S.
Multiple source location: a digital approach.
IEEE Transactions on Aerospace and Electronic Systems, **AES-15** (Jan. 1979), 95–105.

[5] Kumaresan, R., and Tufts, D. W.
Estimating the angles of arrival of multiple plane waves.
IEEE Transactions on Aerospace and Electronic Systems, **AES-19** (Jan. 1983), 134–139.

[6] Schmidt, R. O.
Multiple emitter location and signal parameter estimation.
IEEE Transactions on Antennas Propagation, **AP-34** (Mar. 1986), 276–280.

[7] Barabell, A. J.
Improving the resolution performance of eigenstructure-based direction-finding algorithms.
In *Proceedings of ICASSP*, Boston, MA, 1983, 336–339.

[8] Kaveh, M,. and Barabell, A. J.
The statistical performance of MUSIC and the minimum norm algorithms in resolving plane waves in noise.
IEEE Transactions on Acoustics, Speech, and Signal Processing, **ASSP-34** (Apr. 1986), 331–340.

[9] Rao, B. D., and Hari, K. V. S.
Performance analysis of root-MUSIC.
IEEE Transactions on Acoustics, Speech, and Signal Processing, **37**, 12 (Dec. 1989), 1939–1990.

[10] Roy, R., Paulraj, A., and Kailath, T.
Estimation of signal parameters via rotational invariance techniques—ESPRIT.
In *Proceedings of the 19th Asilomar Conference on Circuits, Systems, and Computers*, Monterey, CA, Nov. 1985.

[11] Roy, R., and Kailath, T.
Total least squares ESPRIT.
In *Proceedings of the 21st Asilomar Conference on Circuits, Systems, and Computers*, Monterey, CA, Nov. 1987.

[12] Evans, J. E., Johnson, J. R., and Sun, D. F.
Application of advanced signal processing techniques to angle of arrival estimation in ATC navigation and surveillance system.
M.I.T. Lincoln Lab., Lexington, MA, Technical Report 582, 1982.

[13] Shan, T. J., Wax, M., and Kailath, T.
On spatial smoothing of estimation of coherent signals.
IEEE Transactions on Acoustics, Speech, and Signal Processing, **ASSP-33**, 4 (Aug. 1985), 806–811.

[14] Pillai, S. U., and Kwon, B. H.
Forward/backward spatial smoothing techniques for coherent signal identification.
IEEE Transactions on Acoustics, Speech, and Signal Processing, **37**, 1 (Jan. 1989), 8–15.

[15] Friedlander, B., and Weiss, A. J.
Direction finding using spatial smoothing with interpolated arrays.
IEEE Transactions on Aerospace and Electronic Systems, **28** (Apr. 1992), 574–587.

[16] Cooper, C. C.
Performance of a switched element direction finding array.
Master's Thesis, The University of Arizona, Tucson, AZ, 2006.

[17] Bethel, R. E., and Bell, K. L.
Maximum likelihood approach to joint array detection/estimation.
IEEE Transactions on Aerospace and Electronic Systems, **40**, 3 (July 2004), 1060–1072.

[18] Johnson, D. H., and Dudgeon, D. E.
Array Signal Processing: Concepts and Techniques.
Upper Saddle River, NJ: Prentice-Hall, 1993.

Wei Wu received the B.S. degree from Fudan University, Shanghai, China in 2005, and the M.S. degree from the University of Arizona, Tucson, in 2007, both in electrical engineering.

From 2006–2007, he was a graduate research assistant in the Laboratory for Sensor and Array Processing in the ECE Department at the University of Arizona. He is currently a DSP engineer with Aware, Inc., Bedford, Massachusetts.

Charles C. Cooper (M'08) received a B.S. in psychology, a B.S. in computer science, and an M.S. in electrical engineering from the University of Arizona, Tucson, in 2002, 2003, and 2006, respectively.

At the University of Arizona, he was a graduate research assistant for the microelectronics design group from 2003 to 2004, and an active member of the Cubesat satellite program from 2001 to 2006. Also in 2006, he was a graduate research assistant for the Laboratory for Sensor and Array Processing. He has worked for Rincon Research Corp. as a digital signal processing engineer since 2004, and is currently a doctoral student in electrical engineering at the University of Arizona. His research interests include application of digital signal processing to RF source localization and array processing.

Nathan A. Goodman (S'98—M'02—SM'07) received the B.S., M.S., and Ph.D. degrees in electrical engineering from the University of Kansas, Lawrence, in 1995, 1997, and 2002, respectively.

From 1996 to 1998, he was an RF Systems Engineer for Texas Instruments, Dallas, TX. From 1998 to 2002, he was a graduate research assistant in the Radar Systems and Remote Sensing Laboratory, University of Kansas. He is currently an associate professor in the Department of Electrical and Computer Engineering, University of Arizona, Tucson. Within the department, he directs the Laboratory for Sensor and Array Processing. His research interests are in radar and array signal processing.

Dr. Goodman was awarded the Madison A. and Lila Self Graduate Fellowship from the University of Kansas in 1998. He was also awarded the IEEE 2001 International Geoscience and Remote Sensing Symposium Interactive Session Prize Paper Award.